ISSN 0021-3640, JETP Letters, 2016, Vol. 103, No. 7, pp. 465–470. © Pleiades Publishing, Inc., 2016.
Original Russian Text © V.A. Maksimenko, V.V. Makarov, A.A. Koronovskii, A.E. Hramov, R. Venckevičius, G. Valušis, A.G. Balanov, F.V. Kusmartsev, K.N. Alekseev, 2016, published in Pis'ma v Zhurnal Eksperimental'noi i Teoreticheskoi Fiziki, 2016, Vol. 103, No. 7, pp. 527–532.

CONDENSED MATTER

Electric-Field Distribution in a Quantum Superlattice with an Injecting Contact: Exact Solution[1]

V. A. Maksimenko[a, b], V. V. Makarov[a], A. A. Koronovskii[b], A. E. Hramov[a, b], R. Venckevičius[c], G. Valušis[c], A. G. Balanov[a, d], F. V. Kusmartsev[d], and K. N. Alekseev[d]

[a] *Yuri Gagarin State Technical University of Saratov, ul. Politekhnicheskaya 77, Saratov, 410054 Russia*
[b] *National Research Saratov State University, ul. Astrakhanskaya 83, Saratov, 410012 Russia*
[c] *Terahertz Photonics Laboratory, Center for Physical Sciences and Technology, LT-01108 Vilnius, Lithuania*
[d] *Department of Physics, Loughborough University, LE11 3TU Loughborough, United Kingdom*
e-mail: K.Alekseev2@lboro.ac.uk

Received February 9, 2016

A very simple model describing steady-state electron transport along a quantum superlattice of a finite length taking into account an arbitrary electrical characteristic of the injecting contact is considered. In the single-miniband approximation, exact formulas for the spatial distribution of the electric field in the superlattice are derived for different types of contact. Conditions under which the field is uniform are identified. Analytical expressions for the current–voltage characteristics are obtained. In the context of the developed theory, the possibility of attaining uniform-field conditions in a diode structure with a natural silicon-carbide superlattice is discussed.

DOI: 10.1134/S0021364016070080

A standard mathematical model describing the spatial distributions of the electric field $F(X)$ and the bulk density of mobile charges $N(X)$ in a one-dimensional solid sample under the conditions of electron injection from a contact includes Poisson's equation and the continuity equation [1]

$$\frac{\partial F}{\partial X} = \frac{q}{\varepsilon_0 \varepsilon_r}(N - N_D), \quad (1)$$

$$J = qNV_d(F) \quad (2)$$

along with the boundary condition for the electric-field strength at the interface between the injecting contact (emitter) and the sample, i.e., $F(X = 0) = F_e(J)$. Here, $X \in [0, L]$ is the coordinate in the solid sample of the total length L, F_e is the field at the contact of a negligibly short length, J is the current density flowing through the entire system including the contact (J is independent of X), $V_d(F)$ is the drift velocity of electrons, $N_D > 0$ is the density of immobile charges, ε_r is the relative permittivity of the sample, ε_0 is the electric constant, and $q = -e$. This simplest model was introduced into solid state physics by Mott and Gurney to describe the impact of space charge on the injection of electrons from an ideal ohmic contact ($F_e = 0$) into an ideal insulator ($N_D = 0$) in the case where the electron mobility is assumed constant ($V_d \propto F$) [2]. A straightforward generalization of the Mott–Gurney model to the case of insulators characterized by a field-dependent differential mobility $\mu_d(F) > 0$ (where $\mu_d = \partial V_d/\partial F$) is now widely used to describe nonuniform field distributions in organic electronic devices [3]. There, typically, the electric field increases steadily from the emitter to the collector.

In semiconductors such as GaAs and InP, in addition to being field-dependent, μ_d can even become negative as a result of intervalley electron transfer. Accordingly, spatial distributions of the field can be quite complicated owing to the possibility of the formation of static charge domains [4]. An important, albeit underestimated, contribution here is a paper by Kroemer [5] motivated by the modeling of the Gunn effect in GaAs under arbitrary boundary conditions. In that paper, it was shown in the context of the most complete variant of the model represented by Eqs. (1) and (2) with $N_D \neq 0$ and $F_e \neq 0$ that not only increasing but also decreasing and, under fairly strict conditions, even spatially uniform distributions of the field can exist.

A quantum superlattice is a specially designed solid lattice where the electron mobility is sufficiently high at least in one direction and the corresponding spatial period considerably exceeds the typical lattice constants of conventional crystals [6, 7]. The impurity

[1] See the supplemental material for this paper at www.jetpletters.ac.ru.

conductivity along the direction of superperiodicity (axis of the superlattice) in such nanostructures originates from the transport of electrons occupying one or several narrow minibands [6, 8]. The majority of quantum superlattices in use are semiconductor heterostructures [6, 9], although, somewhat later, natural superlattices in silicon carbide polytypes have also become the subject of systematic studies [10]. An important property of superlattices is that they exhibit negative differential mobility even in moderate electric fields [6] because of the excitation of relatively long-lived Bloch oscillations in the miniband [11, 12]. The capability of superlattices to amplify and generate electromagnetic waves in the millimeter and submillimeter ranges is likely the most interesting property for applications. This capability can be brought about by various mechanisms, such as moving charge domains [13, 14], Bloch oscillations [15, 16], negative effective mass of electrons [17], and transitions between Wannier–Stark ladders [18]. As a rule, the efficient implementation of these mechanisms requires a nearly uniform field distribution. It should also be mentioned that superlattice microstructures featuring complex nonohmic contacts have recently appeared [19–21]. All of the above makes the problem of predicting the spatial electric-field distribution in superlattice structures an important issue.

Here, we apply the approach of Kroemer [5] to determine the spatial profile of the electric field in a superlattice with an arbitrary injecting contact. We demonstrate that a model of this kind taking into account only one conduction band allows an exact analytical solution. Furthermore, we give a classification of the possible spatial distributions of the field. An important outcome of this analysis is the identification of two simple sufficient criteria for attaining a uniform field distribution for both positive and negative differential mobility of electrons. In both cases, nonohmic contacts are necessary. Using the results obtained, we show that the conditions under which terahertz electroluminescence was recently observed in natural SiC superlattices [16, 20, 22] satisfy our uniform-field criterion.

Following the model described by Eqs. (1) and (2), we consider the spatial distributions of the field $F(X)$ in a superlattice that is uniformly doped with donors to a bulk density of N_D. The field dependence of the electron drift velocity along the superlattice axis is given by the Esaki–Tsu formula [6]

$$V_d(F) = V_0 \frac{F/F_{\rm cr}}{1 + (F/F_{\rm cr})^2}, \tag{3}$$

where $F_{\rm cr} = \hbar/ed\tau$ is the critical field corresponding to the onset of negative differential mobility, $V_0 = \Delta d/2\hbar$ is the maximum electron velocity in the miniband, Δ is the miniband width, d is the period of the superlattice, and τ is the characteristic scattering time. For simplicity, we disregard temperature effects, which can easily be taken into account by the corresponding renormalization of V_0 [7, 9].

It is convenient to introduce the following dimensionless variables (represented by lowercase letters): field strength $f = F/F_{\rm cr}$, current density $j = J/qN_DV_0$, and coordinate $x = X/L$ ($x \in [0, 1]$). Evidently, the Esaki–Tsu critical field and peak current under the electroneutrality condition ($N = N_D$) correspond to $f = 1$ and $j = 1/2$, respectively. Now, combining Eqs. (1)–(3), we obtain

$$\frac{df}{dx} = \alpha\left[\frac{j(1+f^2)}{f} - 1\right], \tag{4}$$

where $\alpha = qLN_D/F_{\rm cr}\varepsilon_0\varepsilon_r$ stands for the dimensionless NL product. Differential equation (4) has two stationary points

$$f_\pm = \frac{1 \pm \sqrt{1-4j^2}}{2j}, \tag{5}$$

corresponding to the two possible values $f(x) = f_+$ and $f(x) = f_-$ of the strength of a spatially uniform electric field that, in principle, can exist in the superlattice. According to Eq. (5), both fixed points are determined solely by the current flowing through the structure. These dependences are illustrated in Fig. 1a. Evidently, the points $f_\pm$ exist only when the total current is lower than the Esaki–Tsu peak current, i.e., $j \leqslant 0.5$. Furthermore, $\mu_d(F_+) < 0$ and $\mu_d(F_-) > 0$; i.e., the values f_+ and f_- belong to the regions of positive and negative differential mobility, respectively.

More complete information on the electric-field distribution can be obtained by integrating Eq. (4) with the boundary condition $f(0) = f_e$, which determines the field strength at the emitter of the structure. As a result, we obtain the formulas (the details of the derivation are given in [23])

$$x_1(f) = \frac{1}{2\alpha j}\left[\frac{1}{\sqrt{1-4j^2}} \times \ln\left(\frac{(1+\sqrt{1-4j^2}-2jf)(1-\sqrt{1-4j^2}-2jf_e)}{(1-\sqrt{1-4j^2}-2jf)(1+\sqrt{1-4j^2}-2jf_e)}\right) + \ln\left(\frac{j-j+jf^2}{j-f_e+jf_e^2}\right)\right], \tag{6}$$

$$x_2(f) = \frac{1}{\alpha j\sqrt{4j^2-1}}\left[\arctan\left(\frac{2jf-1}{\sqrt{4j^2-1}}\right) - \arctan\left(\frac{2jf_e-1}{\sqrt{4j^2-1}}\right)\right] + \frac{1}{2\alpha j}\ln\left(\frac{j-f+jf^2}{j-f_e+jf_e^2}\right), \tag{7}$$

where $x_1(f)$ and $x_2(f)$ should be used for $j < 1/2$ and $j > 1/2$, respectively. When the current approaches the peak value, i.e., $j \to 0.5$, both expressions yield the same result [23]. We also note that, with the use of

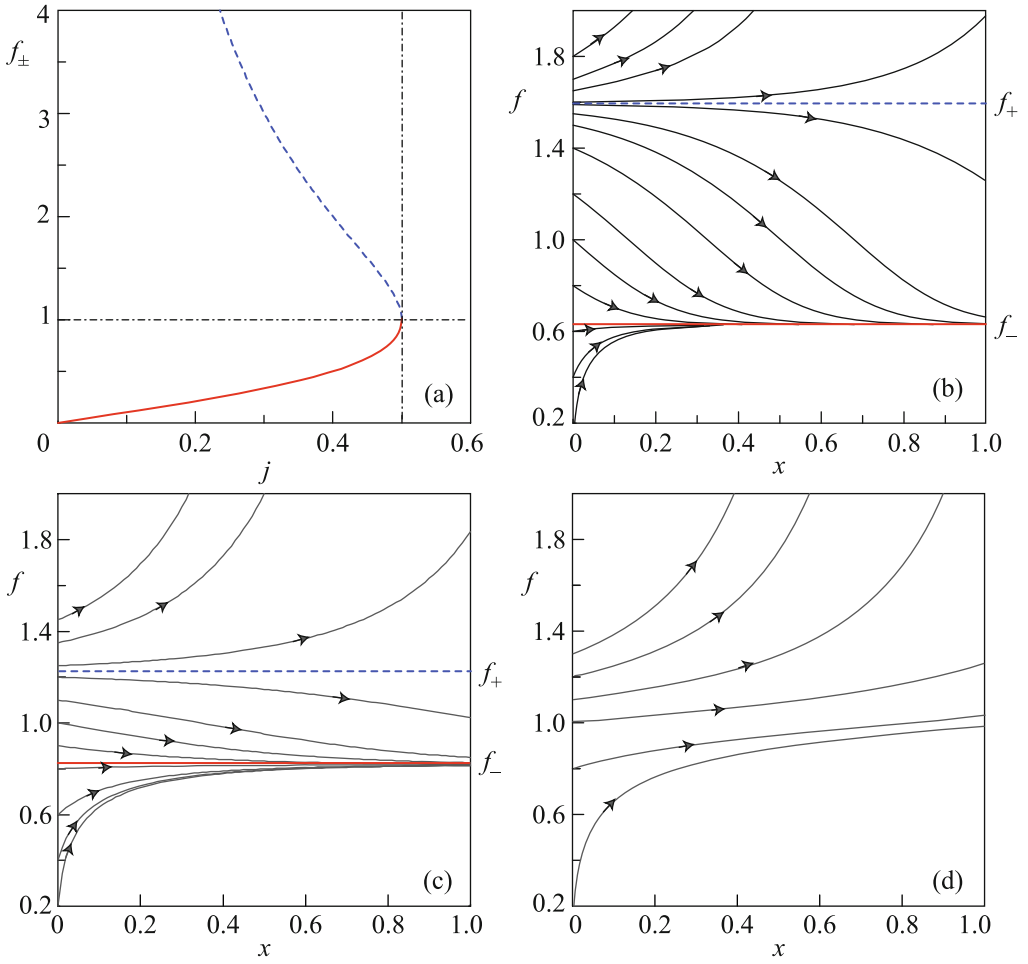

Fig. 1. (Color online) (a) Quantities (red solid line) f_- and (dashed blue line) f_+ versus the current j according to Eq. (5). (b–d) Electric-field spatial distributions $f(x)$ for different field strengths $f_e = f(0)$ at the emitter and the current j = (b) 0.45, (c) 0.49, and (d) 0.505.

Eq. (5), the expression for $x_1(f)$ can be rewritten in the compact and symmetric form

$$x_1(f) = \frac{f_+ + f_-}{\alpha(f_+ - f_-)} \times \left[f_+ \ln\left(\frac{f_+ - f}{f_+ - f_e}\right) - f_- \ln\left(\frac{f_- - f}{f_- - f_e}\right)\right], \quad (8)$$

which demonstrates the importance of the points f_+ and f_- in defining the shape of the spatial distribution of the field for $j < 1/2$.

The spatial distributions $f(x)$ of the electric field plotted according to the obtained exact solutions for different values $f_e = f(0)$ of the field at the emitter and three characteristic values of the current j are shown in Figs. 1b–1d. The calculations were carried out for $d =$ 8.3 nm, $\Delta = 19.1$ meV, $L = 115$ nm, $N_D = 3 \times 10^{16}$ cm^{-3}, and $\tau = 250$ fs; these parameters correspond to the GaAs/AlGaAs superlattice investigated experimentally in [24].

One can see that three types of spatial profile of the field can be implemented in the superlattice for $j < 1/2$. We designate them by roman numerals.

Field distributions of type I occur for $f_e < f_-$. In this case, the field strength increases rapidly with the spatial coordinate and, upon approaching the value of f_-, levels off. We note that, for a low current j, the field is almost uniform along the greater part of the superlattice length (Fig. 1b).

Field distributions of type II are implemented for $f_- < f_e < f_+$. They are characterized by a decrease in the electric-field strength with an increase in the coordinate x. When the current approaches the Esaki–Tsu peak current, points f_- and f_+ converge (cf. Figs. 1b and 1c), and the range of the values of f_e supporting distributions of type II becomes narrower. It is important that, in this situation, the field strength in a type-II distribution decreases with increasing coordinate rather slowly.

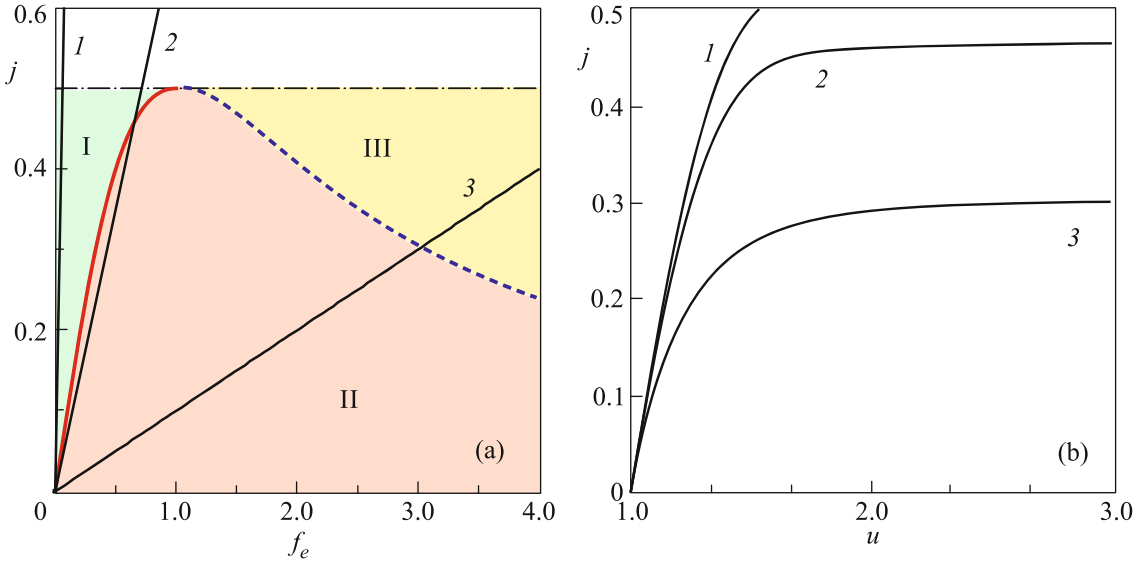

Fig. 2. (Color online) (a) Three regions in the parameter plane $(f_e, j | j \leqslant \frac{1}{2})$ corresponding to the field distributions of types I, II, and III and (red solid and blue dashed lines) the Esaki–Tsu curve along with linear characteristics of emitters with dimensionless conductances $s =$ (*1*) 17, (*2*) 0.7, and (*3*) 0.1. (b) Current–voltage characteristics $j(u)$ of the superlattice corresponding to contact electrical characteristics *1–3*.

Spatial distributions of type III occur for $f_e > f_+$. There, for most of the f_e values, the field strength increases rapidly with the coordinate and can achieve rather high values at the collector of the structure. To obtain a nearly uniform field distribution, the corresponding value of f_e has to be very close to f_+.

Finally, when the current attains the peak value ($j = 1/2$), the points $f_\pm$ merge and disappear, which corresponds to a saddle–node bifurcation. Field distributions taking place for $j > 1/2$ are shown in Fig. 1d. In this case, the field strength increases steadily along the entire length of the system. In agreement with the previously described behavior, this growth is the slowest if the field strength at the emitter is chosen near the superlattice critical field $f_e = 1$. This is explained by the proximity to the bifurcation point.

Until now, we considered the electric field at the emitter f_e and the current j as two independent parameters in the model. However, more typical is a boundary condition that defines the dependence of f_e on the current according to some electrical characteristic of the contact $j = j_{em}(f_e)$ [5]. As an example of such characteristic, we consider the linear dependence $j = sf_e$, where s is the dimensionless conductance of the emitter. On one hand, this model dependence is convenient for describing the transition from an ideal ohmic contact ($s \gg 1$) to a blocking contact ($s \ll 1$) [25]. On the other hand, apart from contacts described by Ohm's law, these linear characteristics describe other types of contact as well [26].

Figure 2a shows three typical contact characteristics (straight lines *1–3*) along with the Esaki–Tsu curve, which represents the ratio of V_d/V_0 in these variables (see Eq. (3)). The Esaki–Tsu curve may be considered as the combination of the curves $f_-(j)$ and $f_+(j)$ (see Fig. 1a). Thus, each point of its intersection with a straight line, where $f_e(j) = f_\pm(j)$, corresponds to those values of the field strength $f(x) = f_e$ and the current that, for a given parameter s, determine the spatially uniform solution. Furthermore, regions I, II, and III on the (f_e, j) plane correspond to the boundary conditions for which the three previously described types of field distribution are implemented. One can see that straight line *1*, which describes an ohmic contact, lies in region I and, thus, cannot intersect the f_+ curve. This illustrates that a uniform field distribution cannot be attained under the conditions of negative differential mobility in a structure with a purely ohmic contact. Straight line *2* (for $j < 0.5$) lies mostly in region II close to the f_- curve and intersects it at $j \approx 0.47$. In this case, both type-I and type-II distributions may occur. Straight line *3*, corresponding to a contact with a low conductance, intersects the f_+ curve at $j \approx 0.3$. There, $f_e > 1$, which corresponds to the condition of negative differential mobility $\mu_d < 0$. Uniform states of this type, which can exist in various quantum superlattices, are of the most physical interest.

In experimental studies [16, 20, 22], terahertz electroluminescence in a 6H–SiC diode microstructure was observed and attributed by the authors to the onset of Bloch oscillations in this natural superlattice. In our

notation, this regime corresponds to $f = \omega_B\tau > 1$, where $\omega_B = \frac{qdF}{\hbar}$ is the Bloch frequency [6]. Intense emission was observed for a current of $I = 210$ mA. For superlattice parameters $d = 0.75$ nm, $\Delta = 260$ meV, $N_D = 10^{16}$ cm^{-3}, the cross-sectional area $S = 3 \times 10^{-5}$ cm^{-2} [16, 20], and $\tau = 3 \times 10^{-13}$ s [27], we have $j = 0.3 < 0.5$ ($j \equiv I/qN_DV_0S$). Then, according to Eq. (5), $f_+ = 3$ or $F_+ = 87$ kV/cm. This value is close to the estimate $F_{rad} = 84$ kV/cm of the field corresponding to the onset of generation obtained in [16] directly from the analysis of the experimental data. Another important fact is that the structure under study had a nonohmic injecting contact in which the nonlinearity of the electrical characteristic was caused by the breakdown of impurity centers. Thus, in spite of a considerable ambiguity in determining the values of F_{cr} and F_{rad}, the emission of terahertz radiation observed in [16, 20, 22] can be quite confidently associated with a transition of the SiC superlattice into a spatially uniform state.

Within the considered model, one can also find the dependence of the voltage drop $U = \int_0^L F(x)dx$ across the superlattice on the current J. Let us introduce the dimensionless variables $u = U/F_{cr}L$ and $f_c = F(L)/F_{cr}$, where $F(L)$ is the field strength at the collector of the structure. Integrating by parts, we obtain [23]

$$u_1(j) = \frac{2(f_c - f_e) + \alpha}{2\alpha j} - \frac{1}{4\alpha j^2}\left[2\sqrt{1-4j^2} \times \operatorname{arctanh}\left(\frac{(f_c - f_e)\sqrt{1-4j^2}}{f_c + f_e - 2j(1 + f_cf_e)}\right) + \ln\left(\frac{j - f_e + jf_e^2}{j - f_c + jf_c^2}\right)\right], \quad (9)$$

and

$$u_2(j) = \frac{f_c - f_e + \alpha}{\alpha j} - \frac{2}{\alpha\sqrt{4j^2 - 1}} \times \left[\arctan\left(\frac{2jf_c - 1}{\sqrt{4j^2 - 1}}\right) - \arctan\left(\frac{2jf_e - 1}{\sqrt{4j^2 - 1}}\right)\right] \quad (10)$$

for $j < 1/2$ and $j > 1/2$, respectively. In turn, the values of f_c are determined by solving the equations $x_{1,2}(f_c) = 1$, where $x_{1,2}(f)$ are defined by Eqs. (6) and (7). The occurrence of the field f_c at the collector in Eqs. (9) and (10) presents some inconvenience when using these formulas. However, this dependence is inevitable in models where spatially nonuniform electric-field distributions are considered [28, 29]. Figure 2b shows the dependences $j(u)$ calculated according to Eq. (9) for superlattice parameters from [24]. Current–voltage characteristics of this shape are typical of various miniband superlattices with no moving charge domains [19, 20, 30].

Thus, in the framework of a well-proven model, we have obtained analytical results that can be used to calculate the spatial distributions of the electric field and current–voltage characteristics in a broad class of superlattice structures. Generalization of these results to the case of a superlattice subjected to a magnetic field is of interest for applications [31, 32].

We are grateful to L. Subačius, T. Hyart, A. Lisauskas, and M.S. Kagan for useful discussions and to H. Roskos for continuing interest in our work and encouragement. This study was supported by the Russian Science Foundation (project no. 14-12-00222). A.G.B. acknowledges support of the Engineering and Physical Sciences Research Council (EPSRC, United Kingdom, grant no. EP/M016099/1).

REFERENCES

1. M. A. Lampert and P. Mark, *Current Injection in Solids* (Academic Press, New York, 1970).
2. N. F. Mott and R. W. Gurney, *Electronic Processes in Ionic Crystals* (Oxford Univ. Press, London, 1940).
3. J. Bisquert, J. M. Montero, H. J. Bolink, E. M. Barea, and G. Garcia-Belmont, Phys. Status Solidi A **203**, 3762 (2006).
4. K. W. Böer, Phys. Status Solidi B **248**, 2775 (2011).
5. H. Kroemer, IEEE Trans. Electron Dev. **15**, 819 (1968).
6. L. Esaki and R. Tsu, IBM J. Res. Dev. **14**, 61 (1970).
7. M. I. Ovsyannikov, Yu. A. Romanov, B. H. Shabanov, and R. G. Loginova, Sov. Phys. Semicond. **4**, 1919 (1970).
8. Zh. I. Alferov, Yu. V. Zhilyaev, and Yu. V. Shmartsev, Sov. Phys. Semicond. **5**, 174 (1971).
9. Yu. A. Romanov, Sov. Phys. Semicond. **5**, 1256 (1971).
10. A. A. Lebedev, Semicond. Sci. Technol. **21**, R17 (2006).
11. K. Leo, P. H. Bolivar, F. Brüggemann, R. Schwedler, and K. Köhler, Solid State Commun. **84**, 943 (1992).
12. V. G. Lyssenko, G. Valušis, F. Löser, T. Hasche, K. Leo, M. M. Dignam, and K. Köhler, Phys. Rev. Lett. **79**, 301 (1997).
13. V. V. Makarov, A. E. Hramov, A. A. Koronovskii, K. N. Alekseev, V. A. Maksimenko, M. T. Greenaway, T. M. Fromhold, O. I. Moskalenko, and A. G. Balanov, Appl. Phys. Lett. **106**, 043503 (2015).
14. I. V. Altukhov, S. E. Dizhur, M. S. Kagan, S. K. Paprotskii, N. A. Khval'kovskii, A. D. Bouravlev, A. P. Vasil'ev, Yu. M. Zadiranov, N. D. Il'inskaya, A. A. Usikova, and V. M. Ustinov, Pis'ma Zh. Eksp. Teor. Fiz. **103**, 128 (2016).
15. C. Waschke, H. G. Roskos, R. Schwedler, K. Leo, H. Kurz, and K. Köhler, Phys. Rev. Lett. **70**, 3319 (1993).
16. V. I. Sankin, A. V. Andrianov, A. O. Zakhar'in, and A. G. Petrov, JETP Lett. **94**, 362 (2011).

17. A. V. Shorokhov, M. A. Pyataev, N. N. Khvastunov, T. Hyart, F. V. Kusmartsev, and K. N. Alekseev, JETP Lett. **100**, 766 (2014).
18. A. A. Andronov, E. P. Dodin, D. I. Zinchenko, Yu. N. Nozdrin, M. A. Ladugin, A. A. Marmalyuk, A. A. Padalitsa, V. A. Belyakov, I. V. Ladenkov, and A. G. Fefelov, JETP Lett. **102**, 207 (2015).
19. L. Subačius, R. Venckevičius, I. Kašalynas, D. Seliuta, G. Valušis, J. Schmidt, A. Lisauskas, H. G. Roskos, K. Alekseev, and K. Köhler, Acta Phys. Polon. A **119**, 167 (2011).
20. V. I. Sankin, A. V. Andrianov, A. O. Zakhar'in, and A. G. Petrov, Appl. Phys. Lett. **100**, 111109 (2012).
21. C. Minot, V. S. Jagtap, E. Galopin, J. C. Harmand, S. Barbay, and J. Mangeney, Phys. Rev. B **91**, 245308 (2015).
22. V. Sankin, A. Andrianov, A. Petrov, A. Zakhar'in, A. Lepneva, and P. Shkrebiy, Nano Res. Lett. **7**, 560 (2012).
23. Supplementary Materials. www.jetpletters.ac.ru.
24. A. E. Hramov, V. V. Makarov, A. A. Koronovskii, S. A. Kurkin, M. B. Gaifullin, N. V. Alexeeva, K. N. Alekseev, M. T. Greenaway, T. M. Fromhold, A. Patanè, F. V. Kusmartsev, V. A. Maksimenko, O. I. Moskalenko, and A. G. Balanov, Phys. Rev. Lett. **112**, 116603 (2014).
25. T. Hyart, N. V. Alexeeva, J. Mattas, and K. N. Alekseev, Phys. Rev. Lett. **102**, 140405 (2009).
26. J. F. Scott, J. Phys.: Condens. Matter **26**, 142202 (2014).
27. V. I. Sankin and A. A. Lepneva, Semiconductors **34**, 803 (2000).
28. H. Kroemer, IEEE Trans. Electron Dev. **14**, 476 (1967).
29. G. S. Gildenblat, A. R. Rao, and S. S. Cohen, IEEE Trans. Electron Dev. **34**, 2165 (1987).
30. A. Sibille, J. F. Palmier, C. Minot, and F. Mollot, Appl. Phys. Lett. **54**, 165 (1989).
31. T. Hyart, J. Mattas, and K. N. Alekseev, Phys. Rev. Lett. **103**, 117401 (2009).
32. T. M. Fromhold, A. Patanè, S. Bujkiewicz, P. B. Wilkinson, D. Fowler, D. Sherwood, S. P. Stapleton, A. A. Krokhin, L. Eaves, M. Henini, N. S. Sankeshwar, and F. W. Sheard, Nature **428**, 726 (2004).

Translated by M. Skorikov